Efficient Usage of RGB-LED for Optical Wireless Communication

Thai-Chien Bui, Saichon Sriphan, and Suwit Kiravittaya*

Advanced Optical Technology (AOT) Laboratory, Department of Electrical and Computer Engineering, Faculty of Engineering, Naresuan University, Phitsanulok, Thailand 65000

* Corresponding author. E-mail address: suwitki@gmail.com

Abstract

Light-emitting diode (LED) can be used as a sensitive optical sensor for a variety of applications. In some applications such as LED-to-LED communication, LED must be able to detect light in visible range. The color of the emitting and sensing LED is an important parameter. In this paper, the influence of LED color in an RGB-LED for optical sensing and emitting in short-range optical wireless communication is investigated. The electrical characteristics of the RGB-LED are analyzed in the static and dynamic response modes. The current-voltage, capacitance-voltage and frequency-dependent capacitance characteristics are measured. From these results, we found that the red color of RGB-LED have the lowest capacitance in reverse biased condition. Therefore, they can be used as an efficient receiver in our proposed visible light range. Performance of RGB-LEDs is then tested with a simple optical wireless communication setup. The results show that only the red and green color of the RGB-LED can efficiently be used for detecting light in visible range. The highest communication speed of 3.5 kbps (with a bit error rate below 10^{-3}) is achieved when the red color LED is used for sensing green light.

Keywords: Light-emitting diode, Visible light communication, Electrical characteristics, Optical communication

Introduction

In the last few decades, apart from general lighting functionalities, light-emitting diodes (LEDs) have been widely investigated in many other applications such as therapy (Miranda, Leal Junior, Marchetti, & Dal Corso, 2014, pp. 359-365), plant growers (Lin, et al., 2013, pp. 86-91), and advanced communication technology (Komine, & Nakagawa, 2004, pp. 100-107; Elgala, Mesleh, & Haas, 2011, pp. 56-62; Gancarz, Elgala, & Little, 2013, pp. 34-41). The usage of visible light LED for high speed communication is considered as a long-term solution of recent congestion in radio frequency spectrum due to the high frequency range of visible light spectrum (400-790 THz). Such a communication system normally refers as visible light communication or Lifi with the requirement of full-duplex communication via visible light and supporting dimming, flickering-free as well as user mobility in the coverage area. In such communication systems, LEDs are mainly used as the data transmitters by simply switching the supply source (voltage/current) in forward biased condition and photodiode is used to detect signal at the receiver. Because of the fast response property of typical solid-state LED, the switching frequency is normally high enough so that human eyes could not perceive the flickering (Brailovsky, & Mitin, 2000, pp. 713-718). The wide use of LEDs is also due to their low-cost, low power consumption, cool operation, long life, and small size.

However, it is noteworthy that LED could also be a cost-effective light sensors operating in a reversed biased condition (Miyazaki, Itami, & Araki, 1998, pp. 547-588; Lau, et al., 2004, pp. 167-173). This interesting property comes from its natural photodiode's behavior of semiconductor PN junction. Under reverse biased conditions, a small induced photocurrent can be generated in the LED structure.

Magnitude of the current is proportional to the intensity of the incident light and typically very small (sub-μA) (Miyazaki, Itami, & Araki, 1998, pp. 547-588). Complicated circuits including low-noise amplifiers and analog-to-digital converter are needed in order to detect the change of incident light intensity when LED is used in this sensing scheme.

An alternative approach for using LED as a sensor is to consider the LED as a diode with a small inherent capacitance when it is operated in reverse biased conditions. The reverse bias voltage then adds up with the built-in potential of the PN junction. This results in the extension of the depletion region, which acts as the light sensing area. With the effect of built-in electric field, the photo-induced electron-hole pairs will be separately swept out of the region and produces the photocurrent (Pierret, 1996, pp. 301-302). The presence of this photocurrent will enhance the discharge of the junction capacitance, which is viewed as a capacitor inside an LED (Dietz, Yerazunis, & Leigh, 2003, pp. 175-191) As a result, by continuously switching between reverse bias (charging) and high-impedance input (discharging) modes while measuring the discharge voltage over the time, LED can be a sensitive and wavelength-selective light sensor (Dietz, & Leigh, 2003, pp. 175-191). Single color LED as optical sensor has been investigated (Dietz, & Leigh, 2003, pp. 175-191; Schmid, Corbellini, Mangold, & Gross, 2013). However, it is expected that the performance of such light sensor devices also depends on its emitted wavelength, the wavelength of incident light and the capacitance in the PN junction.

In this work, we experimentally investigate the performance of an RGB-LED when it is used as a light sensor. The effects of different colors on emitting and sensing light are evaluated. Fundamental electrical characteristics of RGB-LED such as current-voltage relationship and capacitance of each LED under both forward and reverse biased conditions are presented. Those results will then be used to support and explain the observed performance of an optical communication system that uses RGB-LEDs as transceiver. A low-complexity RGB-LED to RGB-LED communication system with low-cost 8-bits microcontroller integrated with built-in ADC is set up in order to evaluate the system performance.

The rest of the paper is organized as follows: In Section II we present the fundamental electrical characteristics of the RGB-LED. In Section III performance of an optical communication system that uses RGB-LED as transceiver is provided and discussed. Our conclusion is in Section IV.

LED Characteristics

An off-the-shelf, diffused RGB-LED, HH-1000CRGBC810W, is selected for our test because of their wide availability and low cost. We evaluate the electrical characteristics of this RGB-LED in two modes, i.e., static response and dynamic response modes. The results are shown in this section.

A. Static Response

Circuit for measuring the electrical characteristics of RGB-LED on static response (i.e. current-voltage (I-V) characteristics) is shown in Figure 1. This circuit consists of a reference resistance R (100 Ω) connected in series with the tested LED. A constant voltage source (V_{DC}) is applied to bias the LED. In our typical test, we sweep the voltages from -5 V to 5 V in order to span in both reverse and forward biased conditions. Typical I-V characteristics of RGB-LED for all three colors in forward bias condition are shown in Figure 2. Tested LEDs are turned on at the diode voltage v_D of about 1.5 V,

2.0 V and 2.3 V for red, green and blue LEDs, respectively. This turn-on voltage generally relates to the band gap energy of LED materials since the band gap defines the wavelength of emitted photons (Parker, 1994; Kasap, 2013). Our result shown in Figure 2 confirms that the tested LEDs have general diode characteristics.

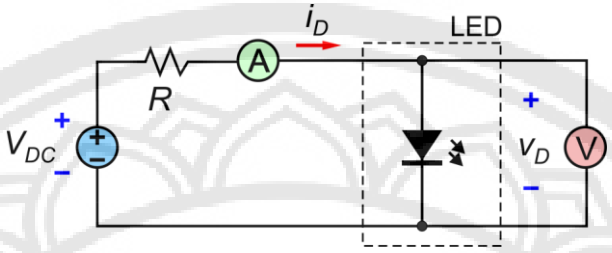

Figure 1 The circuit for measuring static I-V characteristics of an LED.

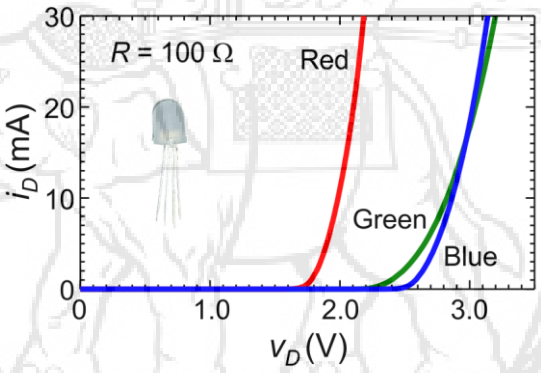

Figure 2 The I-V characteristics of three LEDs in an RGB-LED package. Red, green and blue LEDs show distinct different characteristics. The inset shows a photo of the RGB-LED, which is measured in this work.

B. Dynamic Response

For measuring the dynamic responses of the LEDs, we use a signal-measurement circuit shown in Figure 3. The additional AC voltage source (V_{AC}) provides sinusoidal signal with fixed amplitude A_0 of 400 mV. Large amplitude is applied in order to reduce the effects of noise. Signals are measured by an oscilloscope with the probes channel (Ch.) 1 and Ch. 2 for the AC signal and signal v_D across the LED. In the first test, we fix the AC signal frequency f to 2 MHz and sweep the bias voltage V_{DC} from -20 V to 0 V for measuring the capacitance-voltage (C-V) characteristics. In the second test, we fix the bias voltage V_{DC} at 0 V and sweep the frequencies f from 1 kHz to 100 kHz (with R = 100 kΩ) and 100 kHz to 5 MHz (with R = 1.5 kΩ) for measuring the frequency-dependent capacitance characteristics in low and high frequency ranges, respectively. All measurement is conducted at room temperature (25°C) in dark.

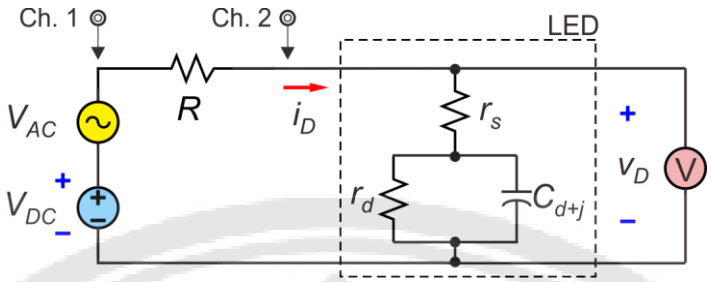

Figure 3 The circuit for measuring the dynamic response of an LED. In the dashed rectangle is an equivalent circuit of the measured LED.

In the analysis of the data from the dynamic response measurement, we consider LED as a small-signal equivalent circuit that is shown in dashed rectangle in Figure 3 (Neamen, 2010, p. 47). In this circuit model, the series resistance r_s is connected in series with the diffusion resistance r_d and the diffusion-junction capacitance C_{d+j}, which are connected in parallel together. For simplicity, we assume r_s = 0 because typical LEDs, which are operated at low injected carriers, show negligible series resistance (Pierret, 1996, pp. 301-302).

In each measurement, raw waveforms from the circuit shown in Figure 3 are recorded. Figure 4 shows the typical waveforms when a constant supply voltage of −5 V and a sinusoidal signal with amplitude A_0 of 400 mV are applied. For extracting the relevant parameters, we fit these data by using *lsqcurvefit* function in MATLAB program (MathWorks, 2013). Amplitude A of the signal across LED and phase difference ϕ between two signals are obtained from these fits. These parameters are related to the C_{d+j} via the circuit model shown in Figure 3. After some algebraic derivations, we can write an expression of C_{d+j} as

$$C_{d+j} = -\frac{A_0 \sin\phi}{\omega R A}, \qquad (1)$$

where $\omega = 2\pi f$ is an angular frequency.

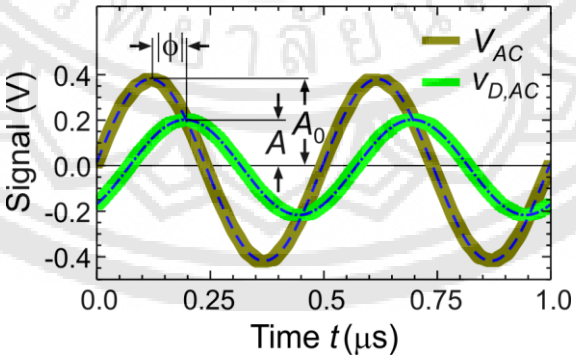

Figure 4 Obtained waveforms from oscilloscope (see Figure 3) when V_{DC} = −5 V, V_{AC} = 400 mV, f = 2 MHz and R = 1.5 kΩ are used. Fitted curves of V_{AC} and v_D are also shown. Signal amplitudes (A_0 and A) and phase difference ϕ can be obtained and used for calculating the LED capacitance value.

The results of dynamic response are shown in Figure 5. The capacitance values are shown as a function of LED voltage v_D for the three LEDs in reverse biased condition. Accuracy of the capacitance measurement depends strongly on the selection of R (See Eq. (1)). With our typical measurement parameters (R = 1.5 kΩ and f = 2 MHz), we obtain an accuracy of ±10%. The measured capacitance values slightly reduce when reverse bias voltages increase. This is due to the enlargement of depletion region (Pierret, 1996, pp. 301-302) Comparing among tested LEDs, we can conclude that the red one has lowest capacitance. Therefore, the red LED should give the fastest response when it is used as a detector. For an LED-LED communication system, we typically bias the transmitter LED in forward condition while the receiver LED is under reverse bias. High-speed responsibility of the detector is important for this system.

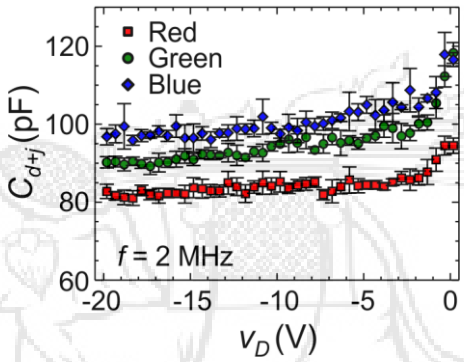

Figure 5 The C-V characteristics of three LEDs under reverse biased conditions.

Advanced optical communication system can operate at wide frequency range. To investigate the frequency-dependent characteristics of LEDs, we therefore sweep the AC signal frequency in the range between 1 kHz and 5 MHz. A constant voltage V_{DC} of 0 V is also applied for zero-biasing the LED. The frequency-dependent capacitance values of each LED are shown in Fig. 6. Red LED shows the lowest C_{d+j} value in all frequency ranges. This implies rather constant junction capacitances in the tested LEDs. Note that different resistors are used in different frequency ranges in order to reduce uncertainty in phase extraction from the signals (See Eq. (1) and Figure 4).

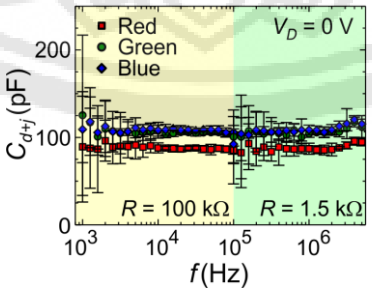

Figure 6 The frequency-dependent capacitance characteristics of three LEDs in low frequency (1 kHz to 100 kHz) and high frequency (100 kHz to 5 MHz) ranges. A constant V_{DC} of 0 V is applied during the measurement.

From the experimental results shown in this section, we can conclude that the red LED is suitable for using as a light sensor (or receiver) in LED-LED communication system. Another consideration must be included. According to the absorption/emission theory of semiconductor materials, red LED is the best for general light sensor because it will also absorb the shorter wavelength lights (blue and green). However, not all shorter wavelength light will be good absorbed by the red LED. Miyazaki, Itami, & Araki. (1998, pp. 547-588) reported the overlapping effect between extinction and absorption spectra of red and blue LEDs. They found that when red LED is used as a detector, it can absorb shorter-wavelength light more effective than other light wavelength. Results from our work are consistent with their report.

RGB-LED To RGB-LED Communication System

In the previous section, the basic electrical characteristics of individual RGB LEDs are presented. We showed RGB-LED's behaviors when it is activated in static and dynamic modes. From the frequency-dependent capacitance measurement at low frequency, red and green LEDs are suggested to be a good receiver and transmitter, respectively. In this section, we will demonstrate a practical usage of these LEDs in a low-cost communication system using RGB-LED as transceiver.

A. Low-Complexity Communication Circuit

Communication system using sophisticated circuits can achieve high bit rates. However, for some specific applications that require not-too-high data rate, it is preferred to use low-complexity system with low-cost and widely available devices. In this work, an off-the-shelf 8-bit microcontroller (ATmega328P) (Atmel, 2009) with built-in 10-bit precision ADC is used to drive two RGB-LEDs, one for transmitting optical pulse and the other for receiving. Figure 7 illustrates our target test-bed whereby transmitter and receiver are on two independent circuit broads.

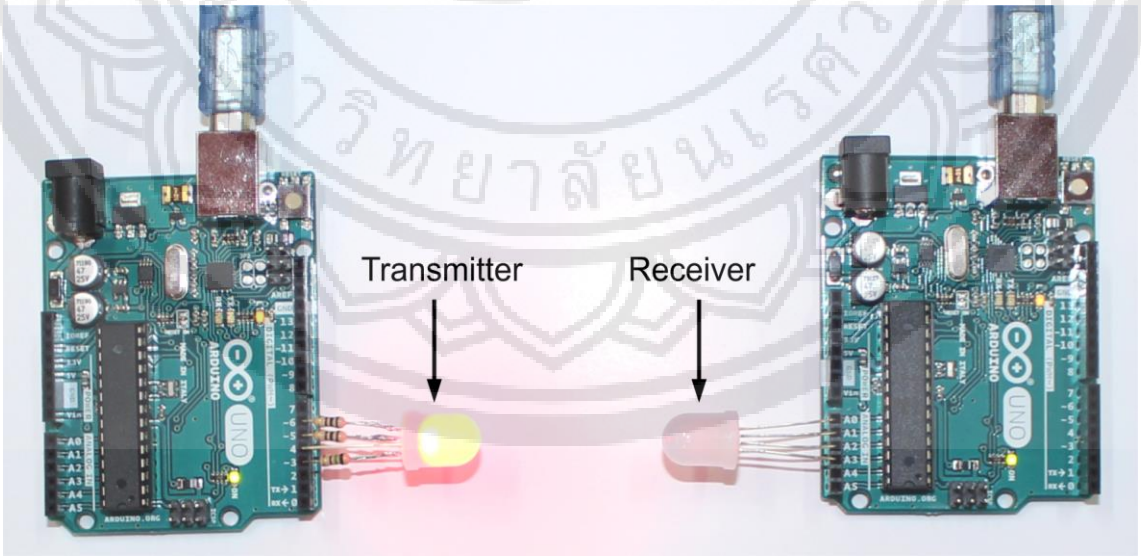

Figure 7 RGB-LED communication set up

At the transmitting end, three different current-limiting resistors of 150 Ω, 100 Ω, and 100 Ω, are soldered in series with red, green, and blue pins of the RGB-LED respectively. Those resistors are chosen in the way so that the injecting currents through all three anode pins are 20 mA, which is the recommended typical current of the RGB-LED. All four pins including cathode pin are then hooked up with 4 digital pins of microcontroller and transmits optical pulse at pre-determined frequency and duty circle. It is assumed that the transmitted frequency f_0, is known at the receiver and the duty circle is set to 50% for all frequencies by default.

Unlike the transmitter, RGB-LED at the receiving end is directly connected with four analog pins of microcontroller as shown in Figure 7. A built-in timer/counter with an internal clock f_{CLK} of 16 MHz and the default prescaler of 64 is enabled at clear timer on compared modes. Hence, every $1/f_0$ period of time, an interrupt is triggered. In the interrupt, firstly, the RGB-LED is reversed-biased for 10 μs for charging up the capacitance to around 5V. Hence the cathode pin of LED will be set to high-impedance input mode and the RGB-LED will slowly discharge afterwards. After finishing the interrupt, the timer starts to count for another $1/f_0$ period of time. While waiting for the next interrupt, an ADC at auto trigger mode is used to continuously measure the discharge voltage of the RGB-LED and stored it into two 8-bit registers. Generally, this two 8-bit data will be converted back to 10-bit integer before transferring it out via serial communication to the computer. However, this conversion process requires quite a long period of time. Hence, we print this two 8-bit data directly to the computer and do the conversion in the computer. This will minimize the time needed for reading and writing one data and maximize the number of data can be sampled within $1/f_0$ period of time. The achievable sampling time is around 80 μs, given a sample rate of 12500 samples per second. When the timer is reached another $1/f_0$ period of time, measuring and writing data is paused and the interrupt is triggered again. This process is continuously repeated over the time. It is noteworthy that by connecting the oscilloscope probe to the cathode of the RGB-LED, a higher sampling rate can be achieved. However, the oscilloscope probes will make the capacitance discharge faster than normal (Giustiniano, Tippenhauer, & Mangold, 2012, pp. 1-8). For this reason, we implement the sampling process in the microcontroller instead of using an external oscilloscope.

B. Communication Performance

All the measurements are done in the dark environment in order to avoid the effects of ambient light. The communication distance between emitting and receiving LED is set to 3 cm. Figure 8 illustrates the transmitted and received waveforms of four Rx modes at the bit rate of 1 kilobit per second (kbps). Referring to Figure 8, it is clear that the received waveforms at different Rx modes have color dependent behaviors as expected. When all red, green and blue pins at the receiving RGB-LED are under reverse biased condition (so-called Rx-RGB mode) the received waveform for Tx-green and Tx-blue modes are almost similar. The discharge speed is slightly slower when red light is used at the transmitter side (Tx-red). At the end of each discharge period when a symbol "1" is transmitted, the remaining voltage in case of Tx-red is approximately 0.05 V higher than Tx-green and Tx-blue modes. However, this gap between Tx-red and two other modes is significant when only the red pin at the receiving LED is under reversed condition (Rx-red) as illustrated in Figure 8(b). In this case, the average voltage drops within 1 ms of Tx-green is greatest to about 4.48 V while Rx-red and Rx-blue

are to about 4.7 V and 4.79 V, respectively. This improvement of using red color LED for detecting green light is due to the absorption of red LED is shifted to the higher energy (green region) (Miyazaki, Itami, & Araki, 1998, pp. 547-588) and hence the overlap between emission and absorption spectra of red color are mainly in the wavelength range of green. Although the Rx-red mode performs a good received waveform for Tx-green and Tx-red, the Rx-RGB mode is sufficient for the application that requires detecting all the colors at the same performance.

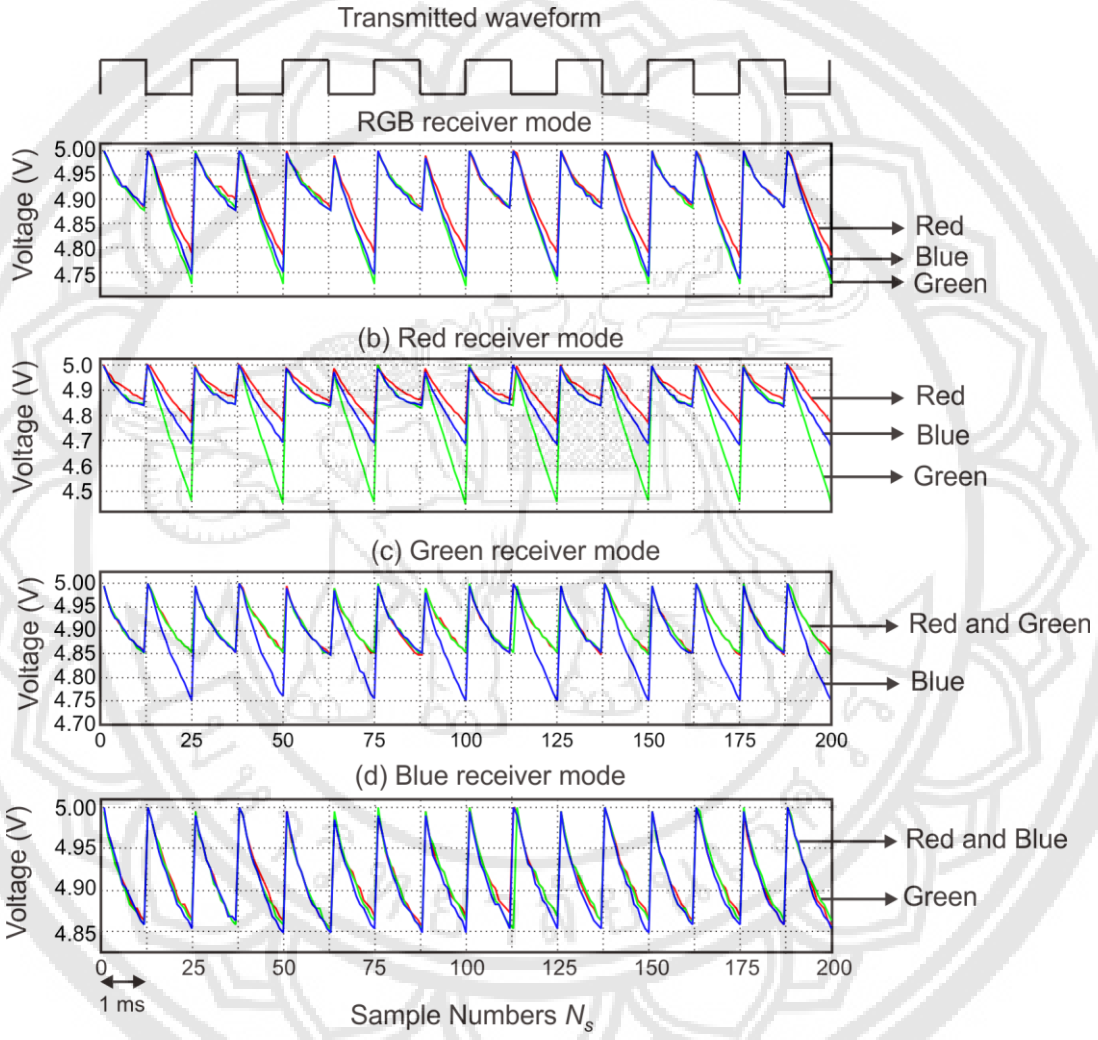

Figure 8 Transmitted and received waveform of RGB-LED in (a) RGB receiver (or Rx-RGB) mode, (b) red receiver (or Rx-red) mode, (c) green receiver (or Rx-green) mode and (d) blue receiver (or Rx-blue) mode.

Using LED for sensing light has the wavelength selective property since only the light with sufficient energy can excite the photo-current in the LED under reversed biased condition. This wavelength-selective property is shown clearly in the Figure 8(c) and (d) where the green and blue LEDs are the detectors. In the case of Rx-green mode (Figure 8(c)), the red and green incident lights are out of sensing range. Meaning that the discharge speed is remained the same for both symbols: "1" and "0" for both red

and green transmitted lights. It can be explained based on the fact that absorption spectrum of the green LED is shifted to the blue region (to higher energy range). Hence, only the incoming blue light that has shorter wavelength than green light can be sensed in the Rx-green mode. However, this blue light is no longer be sensed at Rx-blue mode and that all the incoming light with colors of red, green and blue are out of sensing range. This is because the blue LED is only sufficient to detect light in the UV range (Miyazaki, Itami, & Araki, 1998, pp. 547-588). This wavelength selective property hinders us to use blue LED as a visible light sensor.

To further evaluate the performance, we use the threshold method to decode each received waveform and compare with the transmitted waveform to obtain the bit error rate under varying the data rate. First, the sampling number, N_S , over $1/f_0$ period of time is given as

$$N_S = 12500\frac{1}{f_0}, \qquad (2)$$

where f_0 is the transmitted frequency and 12500 is sampling rate of the built-in ADC of microcontroller. Hence, after sampling around N_S data points the remained discharge voltage v_R is measured. This voltage is compared with a pre-defined optimal threshold V_{TH}, and the decision at made as:

$v_R > V_{TH}$ → transmitted symbol is "0"

$v_R < V_{TH}$ → transmitted symbol is "1"

Figure 9 shows the bit error rate (BER) plots for three different receiving configurations those are Rx-RGB, Rx-red, and Rx-green. The green color at the transmitting side (Tx-green) are selected to plot the BER for both Rx-RGB and Rx-red modes since the green light performs fastest discharge speed as shown in Figure 8 and the blue color are used in Rx-green mode. For every configuration, 500000 data points are recoded for analyzing at various bit rates from 2 kbps to 4.5 kbps. All the BER plots show a typical trend of BER versus data rate (Haigh, Ghassemlooy, Rajbhandari, & Papakonstantinou, 2013, pp. 148-154). Referring to Figure 9, the BER is lowest when Tx-green and Rx-red modes are used. The achievable data rate of this configuration at BER of 10^{-5} is 3.5 kbps, and at BER of 10^{-2} is 4 kbps. This achievable data rate is much lower for Tx-green and Rx-RGB configurations (about 2.1 kbps and 2.8 kbps at BER of 10^{-5} and 10^{-2}, respectively). When Rx-green is used, it detects the blue light at only very low data rate. This is due to the low intensity of blue light of the tested RGB-LED. As a result, when Rx-green is used, the BER is very high at data rate larger than 2.5 kbps and reaches to 10^{-1} BER at only 3 kbps. Our experiments also reveal that the performance of all configurations is saturated at high data rate due to the limited processing of the low-cost microcontroller in this set up.

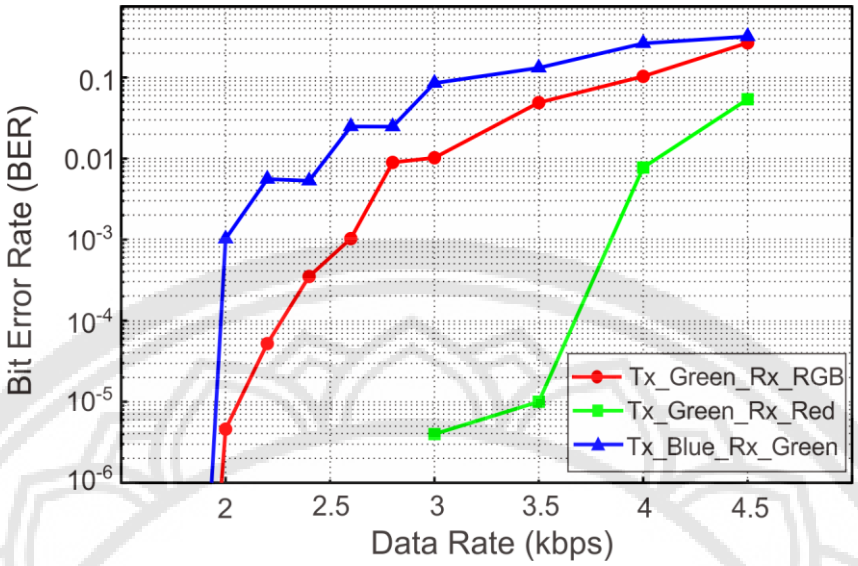

Figure 9 Observed BER performances of an LED-LED communication system for green transmitter and RGB receiver (Tx_Green_Rx_RGB), green transmitter and red receiver (Tx_Green_Rx_Red) and blue transmitter and green receiver (Tx_Blue_Rx_Green).

Conclusion

Using LED as visible light sensor for short-range free space optical communication has several advantages and can be applied in a variety of applications. This paper investigates the performance of using RGB-LED as light sensor by demonstrating their fundamental electrical characteristics and applying it in a LED-LED communication system, whereby RGB-LED is used for both transmitting and receiving visible light signal. For electrical characteristics, we evaluated the static and dynamic responses of this device and found that red LED has lowest capacitance value. When using the LEDs in an LED-LED communication system, we found that red LED is suitable for using as a receiver and green LED is more suitable for using as a transmitter. From our results, only appropriated colors can be used in such system due to the wavelength selective property the LED. This work will enhance the usability of LED as a simple light sensor in many applications.

Acknowledgements

The authors gratefully acknowledge Dr. Keattisak Sripimanwat for his fruitful information on the visible light communications and Assistant Professor Dr. Akaraphunt Vongkunghae and Mr. Tanee Kosum for their technical support. This work is financially supported by Naresuan University and the Faculty of Engineering, Naresuan University.

References

Atmel. (2009). 8-bit Atmel microcontroller with 4/8/16/32K bytes in-system programmable flash. Retrieved November 24, 2015, from http://www.atmel.com/images/atmel-8271-8-bit-avr-microcontroller-atmega48a-48pa-88a-88pa-168a-168pa-328-328p_datasheet_summary.pdf

Brailovsky, A. B., & Mitin, V. V. (2000). Fast switching of light-emitting diodes. *Solid-State Electronics*, 44, 713-718.

Dietz, P., Yerazunis, W., & Leigh, D. (2003). Very low-cost sensing and communication using bidirectional LEDs. In A. K. Dey, A. Schmidt, & J. F. McCarthy (Eds.). *UbiComp2003: Ubiquitous Computing.* (pp. 175-191). Springer-Verlag: Berlin Heidelberg.

Elgala, H., Mesleh, R., & Haas, H. (2011). Indoor optical wireless communication: Potential and state-of-the-art. *IEEE Communications Magazine*, *49*(9), 56-62.

Gancarz, J., Elgala, H., & Little, T. D. C. (2013). Impact of lighting requirement on VLC systems. *IEEE Communications Magazine*, *51*(12), 34-41.

Giustiniano, D., Tippenhauer, N. O., & Mangold, S. (2012). Low-complexity visible light networking with LED-to-LED communication. IEER: Wireless Days (WD), 2012 IFIP.

Haigh, P. A., Ghassemlooy, Z., Rajbhandari, S., & Papakonstantinou, I. (2013). Visible light communications using organic light emitting diodes. *IEEE Communications Magazine*, *51*(12), 148-154.

Kasap, O. (2013). *Optoelectronics and Photonics: Principles and Practices*, New Jersey: Prentice Hall.

Komine. T., & Nakagawa, M. (2004). Fundamental analysis for visible-light communication system using LED lights. *IEEE Transactions on Consumer Electronics*, *50*(1), 100-107.

Lau, K. T., Baldwin, S., Shepherd, R. L., Dietz, P. H., Yerzunis, W. S., & Diamond, D. (2004). Novel fused LED's devices as optical sensors for colorimetric analysis. *Talanta*, 63, 167-173.

Lin, K. H., Huang, M. Y., Huang, W. D., Hsu, M. H., Yang, Z. M., & Yang, C. M. (2013). The effects of red, blue, and white light-emitting diodes on the growth, development, and edible quality of hidroponically grown lettuce (Lactuca sativa L. var. capitata). *Scientia Horticulturae*, 150, 86-91.

MathWorks. (2013). *MATLAB Programming Fundamentals*. Natick, MA: The MathWorks.

Miranda, E. F., Leal Junior, E. C., Marchetti, P. H., & Dal Corso, S. (2014). Acute effects of light emitting diodes therapy (LEDT) in muscle function during isometric exercise in patients with chronic obstructive pulmonary disease: preliminary results of a randomized controlled trial. *Lasers in Medical Science*, 29, 359-365.

Miyazaki, E., Itami, S., & Araki, T. (1998). Using a light-emitting diode as a high-speed, wavelength selective. *Review of Scientific Instruments*, *69*(11), 547-588.

Neamen, D. A. (2010). *Microelectronics: Circuit Analysis and Design*, Singapore: McGraw-Hill.

Parker, G., (1994). *Introductory Semiconductor Devices Physics*. London: Prentice Hall.

Pierret, R. F. (1996). *Semiconductor Device Fundamentals*. Reading, MA: Addison Wesley.

Schmid, S., Corbellini, G., Mangold, S., & Gross, T. R. (2013). LED-to-LED visible light communication networks. *Proceedings of the 14th ACM International Symposium on Mobile Ad Hoc Networking and Computing*, 1-9. Retrieved November 24, 2015, from http://www. disneyresearch.com/wp-content /uploads/p1- schmid1.pdf